energies

MDPI

Review

Critical Review of EMC Standards for the Measurement of Radiated Electromagnetic Emissions from Transit Line and Rolling Stock

Andrea Mariscotti

Department of Electrical, Electronics and Telecommunication Engineering and Naval Architecture (DITEN), University of Genova, 16145 Genova, Italy; andrea.mariscotti@unige.it

Abstract: Accurate and comprehensive methods for the assessment of radiated electromagnetic emissions in modern electric transportation systems are a necessity. The characteristics and susceptibility of modern victim signaling and communication radio services, operating within and outside the right-of-way, require an update of the measurement methods integrating or replacing the swept frequency technique with time domain approaches. Applicable standards are the EN 50121 (equivalent to the IEC 62236) and Urban Mass Transport Association (UMTA) with additional specifications from project contracts. This work discusses the standardized methods and settings, and the representative operating conditions, highlighting areas where improvements are possible and opportune (statistical characterization of measurement results, identification and distinction of emissions and line resonances, and narrowband and broadband phenomena). In particular for the Electromagnetic Compatibility (EMC) assessment with new Digital Communication Systems, the characterization of time distribution of spectral properties is discussed, e.g., by means of Amplitude Probability Distribution and including time distribution information. The problem of determination of site and setup uncertainty and repeatability is also discussed, observing on one hand the lack of clear indications in standards and, on the other hand, the non-ideality and intrinsic variability of measurement conditions (e.g., rolling stock operating conditions, synchronization issues, and electric arc intermittence).

Keywords: antennas; electromagnetic compatibility; electromagnetic radiation; measurement standards; railway transportation; repeatability; reproducibility; transients; uncertainty

Citation: Mariscotti, A. Critical Review of EMC Standards for the Measurement of Radiated Electromagnetic Emissions from Transit Line and Rolling Stock. *Energies* **2021**, *14*, 759. https://doi.org/10.3390/en14030759

Academic Editor: Chunhua Liu
Received: 23 December 2020
Accepted: 28 January 2021
Published: 1 February 2021

1. Introduction

Electrified transportation systems may represent a significant source of radiated electromagnetic emissions with peculiar mechanisms of emissions [1–6], considering disturbance to both circuits and services within the right-of-way [7–15], and more generally to the "outside world" [16,17]. The intensity of electromagnetic field emissions and equipment exposed, and potentially interfered with may vary depending on the frequency interval. At low frequency (e.g., traction supply fundamental and harmonics), intensity and propagation may affect systems at some distance from the right of way (hospitals, laboratories, etc.). With increasing frequency, the propagation distance reduces and attention is focused on systems that are part of the transportation system itself and operate both onboard and trackside (mainly signaling and communication systems). The measurement procedure, thus, should consider the characteristics and susceptibility of such victim systems, e.g., selecting data sampling, detection, and post-processing criteria suitable for modern digital radios, rather than old AM and FM broadcasting [18].

Recently, the measurement of electromagnetic emissions from electric transportation systems is commonly carried out in compliance to the CENELEC EN 50121 standards (equivalent to the IEC 62236): EN 50121-2 [16,17] for line and substation emissions and

50121-3-1 [19,20] for rolling stock emissions. They appeared first about 25 years ago (1996) to address emerging Electromagnetic Compatibility (EMC) problems at that time:

- disturbance to radio and TV services with some episodes of interference in the 1980s related to the new high-speed lines and modern trams amid cities, urging for standardization;
- equipment onboard and wayside needed specific test levels to cope with the severity of the electromagnetic environment and functional safety requirements set forth by the EN 50129 [21], issued first in 1998, and EN 61508-2 [22], appearing in 2002.

The EN 50121 has undergone four major revisions (1996, 2000, 2006, and 2015) and the 2015 edition was repeated in 2016/2017. Whereas specifications for testing of equipment immunity have improved almost at each edition, the assessment of emissions has not seen a similar progress: limits sometimes have been relaxed and frequency intervals reduced, as well as requirements for definition of operating and measurement conditions have set back, ending up with several degrees of freedom and a larger uncertainty [23].

The second major reference is the Urban Mass Transport Association (UMTA) test procedures [24,25], augmented and then de facto replaced by the contractual specifications of each transportation project [26]. Technically speaking, UMTA procedures find its ground in Holmstrom's work [27] and in the MIL-STD-461, now at rev. G [28].

Electric transportation systems have grown and serve more and more often densely populated city centers: tramlines, light rail transits, metros, and commuter and high-speed railways, but also other similar applications using a current collection system (trolleybuses and streetcars). Onboard propulsion and auxiliaries, as well as substations, see a widespread use of power conversion devices [29,30], with common-mode and radiated emissions shifted to higher frequency by the use of faster semiconductors. They are the first victim environment for their own emissions interacting and possibly affecting the modern signaling, control, and communication systems, based on a wide range of known (e.g., GSM (the Global System for Mobile Communication), Wi-Fi) and innovative (e.g., CBTC, that stands for Communications-Based Train Control) protocols.

Radio services for communication and broadcasting have increased in number and complexity, with a wide range of operating bands, protocols, and exigencies of quality of service [31–37], and many are candidates for prospective railway radio signaling implementations.

In addition, other radio services serve specific purposes of guidance and control, implementing often safety-related functions, such as Instrumental Landing System [3] and DVOR (Doppler Very-high-frequency Omni Range), guiding with direction and distance information for aircraft landing, for both en route and take off. For railways and metros there is a significant effort beyond CBTC to exploit more modern Long Term Evolution (LTE) between 450 MHz and 2 GHz (basically using optimized code handbooks and multiple antennas managed by smart algorithms [36]). Wi-Fi-based train-wayside communication sees an increasing demand for throughput and availability, especially to support passengers' connection, broadcasting services, and video surveillance [32,34]. Procedures and methods for assessment of electromagnetic emissions and interference should thus keep the pace of this technological progress.

Low-frequency magnetic emissions at dc, fundamental, and harmonics are not considered here, as methods are different, but well established, as demonstrated for modeling and measurements [38,39], and considered extensively to evaluate (e.g., interference to medical equipment [40]).

This work focuses on methods and relevant factors for complete, accurate, and repeatable measurements to assess rolling stock and line radiated emissions in view of the characteristics of the potential victims. In particular, the discussion encompasses the distinction of narrowband and broadband phenomena, the identification and influence of line resonances and transients, the rapidity of the frequency sweep compared to vehicle dynamics, and in general repeatability, reproducibility, and uncertainty. It is shown that a significant contribution may come by the use of time-domain methods, as well as Ampli-

tude Probability Distribution (APD) and joint time-frequency transformation, to estimate the impact on modern digital radio receivers.

The work is organized as follows. Section 2 focuses on the existing EMC standards for railway applications and prescriptions in terms of measurement parameters (limit curves, frequency, distance, and resolution bandwidth). Section 3 discusses measurement scenarios, operating conditions and characteristic of the system that have influence on the measurement results and their variability, or uncertainty. Section 4 then discusses the most suitable measurement techniques and settings in light of the previous two sections, in order to improve uncertainty, repeatability, and statistical significance of measurements, thus improving the profitability and reliability of the so-obtained representation of radiated electromagnetic field emissions.

To guide the reader through the discussion and the relevant outcomes, the main facts and conclusions are reported in the "synthesis and highlights" subsection as a list of the major points, related methods, and suggested precautions and improvements.

2. Test and Measurement Scenario

EN 50121 and UMTA both specify testing of vehicle using traction, coasting and braking modes: the EN 50121 provides, however, more details as for speed and effort to apply. They agree also that acceleration and braking must be applied when passing in front of the antenna (see Section 3.1). The UMTA standard does not require line measurements. Section 2 considers the main distinctive elements of the two sets of standards and prepares the discussion of Section 3 on weak points and improvement.

2.1. Overall Frequency Range

Historically, the development of the EN 50121 [16–20] focused mainly on intermittent emissions of the pantograph electric arc, implicitly encompassing the emissions from power converters. Although the initial demonstration in the CENELEC working documents included time-domain recordings, the frequency-domain measurement has since been kept as the preferred method, in line with other EMC standards for electrical and electronic products [41,42], which establish for radiated emissions a frequency interval starting from 30 MHz. The EN 50121 extends now [17,20] the interval for radiated emissions down to only 150 kHz, whereas the 2006 version [16,19] extended to 9 kHz. The upper limit for EN 50121 is always 1 GHz, although the exigency of demonstrating compatibility with modern communication technologies is compelling (mobiles in 2.1 and 2.4 GHz bands, signaling and telecom using 2.4 and 5 GHz commercial bands and the latest 5G technology) [2,12].

UMTA standards in 1987 [24,25] had initial prescriptions for 140 kHz–400 MHz, with suggested expanded intervals of 14 kHz–30 MHz with H-field limits and 400 MHz brought to 1 GHz. These standards did not indicate limits and were never updated after 1987 (a draft around 2000 was not applied). Nevertheless, frequency ranges down to 10 kHz and up to 6 and 7.5 GHz were included in specifications [26].

The intermediate subdivision of frequency ranges is discussed in Section 2.5 in relation to prescriptions for antennas.

2.2. Limits

UMTA standards [24,25] specify limits of E-field, suggesting expanded H-field measurements. Modern railway projects refer in general to EN 50121 with limits expressed in H-field values for the lower frequency interval (0.009–30 MHz in 2006, reduced to 0.15–30 MHz in 2015) and E field above 30 MHz. Despite the reduction of the frequency interval, the H-field relevance was confirmed, considering induction and disturbance in exposed circuits, and propagation at longer distance thanks to the lower wave impedance, however, an H-to-E field conversion factor for reactive and near-field conditions has not been provided.

Limits are shown in Figure 1, having expressed EN 50121 values in dBµV/m/MHz, with equivalent E-field for 100 ft distance (assuming conversion in far field conditions, so

using the free space characteristic impedance Z_0 of 377 Ω, or +51.5 dB, and the correction of thee field intensity at various distances is considered in Section 2.3). It is apparent that EN 50121 is more permissive at low frequency, although the transformation of H-field by Z_0 is overestimating, being emissions in the reactive region and thus with a lower wave impedance. There is better agreement between limits above about 30 MHz.

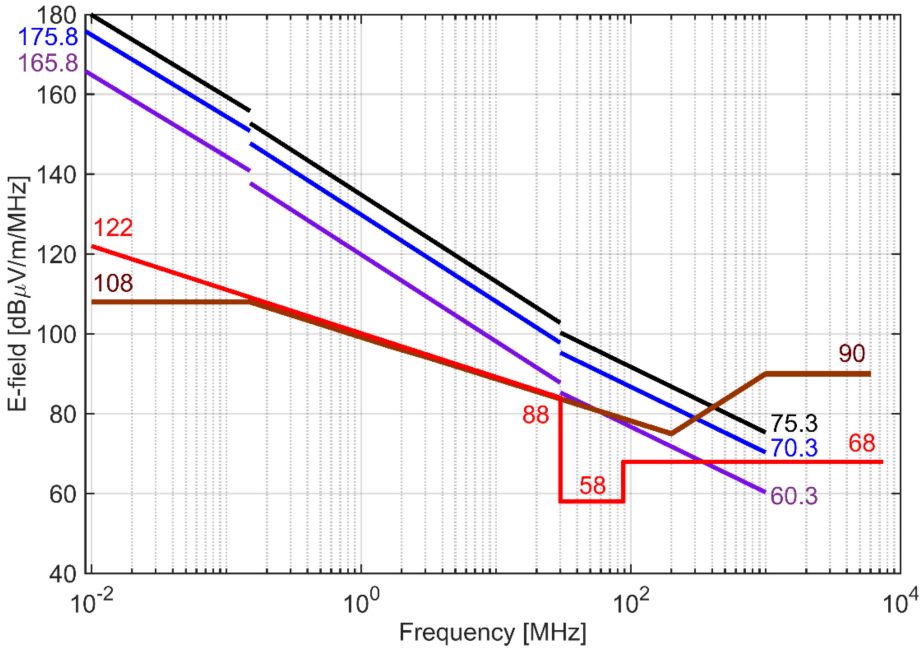

Figure 1. Limits as E-field per MHz at distance of 100 ft (far field calculation from H-field by applying the +51.5 dB correction; linear with respect to Resolution Bandwidth (RBW)): EN 50121-3-1 dynamic Peak limits for railways (black), metros (blue), trams (violet); New York R211 (red); Los Angeles HR4000 (brown).

Stipulation of limits is a complex process that should consider the victim radio services and the radiation efficiency of the emitting elements, i.e., vehicle body, electric arc, and pantograph, but most of all the catenary system. The latter can be modeled and behaves like a long wire antenna [43], fairly efficient over the MF and HF range (Medium Frequency and High Frequency as in ITU-T definition, between 0.3 and 30 MHz), where various services operate (radiolocation, maritime mobile, radio navigation, amateur radio, and broadcasting) [44]. Third rail systems have lower radiation efficiency for two reasons: the height of the third rail above top of rail (and thus the emitting loop area) is less than 1/10 of that for catenary systems; the coupling capacitance to the running rails and ground, as a consequence, is larger. Calculation using the method of potential [45,46] reports a per-unit-length capacitance of 8–9 pF/m for catenary systems 15–16 pF/m for a third rail systems in single-track configuration. For double-track configurations the two capacitance values increase to about 11–12 pF/m for catenary systems and 16–17 pF/m for third rail systems. A larger capacitance implies lower characteristic impedance and a larger displacement current at high frequency, shunting the components injected into the traction supply line and reducing the effective length of the long wire antenna represented by the traction supply line itself.

Limits were defined for both continuous and transient phenomena at once [8], but they have much different effect on radio systems: disambiguation is an issue that in frequency domain was addressed by the use of different detectors. As in Section 4, the use of time-domain methods with suitable victim receiver characterization is recommended.

2.3. Measurement Distance

With the significant extension of the source (vehicle, line, and substations) and the variable nature of the electromagnetic (e.m.) field depending on frequency, distance, and soil properties, extrapolation of field intensity at different distances and locations is troublesome [47]. Measurement distances were selected as compromise between source size and a desirably large signal-to-noise ratio (the farther from the source, the lower the expected intensity), as observed in [47], Section II, [48]:

- The EN 50121-2 and -3-1 prescribe a r^* = 10 m distance and at other distances the electric field intensity is extrapolated to the 10 m reference distance with a linear path loss (typical of far field conditions) including a correction coefficient (1). The correction in principle depends on several factors, such as the relationship between wavelength, distance, and height above ground, and ground reflected terms, that in turn depend on the ground shape (flat, rough, and wet) and soil resistivity. The standard or related publications do not clarify, however, how these exponent values for the path loss equation were determined and what is their variability.
- UMTA sets two distances r^*(UMTA) with two different limit curves: 50 feet (15.2 m) and 100 feet (30.5 m), and no extrapolations or corrections are allowed.

$$E[10\text{m}] = E[x] + n\{\ 20\log_{10}(x/10)\ \} \quad (1)$$

The coefficient n is given in Table 1 of the EN 50121-2 and is equal to the following values: 1.8 for frequency between 0.15 and 0.4 MHz, 1.65 between 0.4 and 1.6 MHz, 1.2 between 1.6 and 110 MHz, and 1.0 above 110 MHz (up to the maximum frequency covered by the standard that is 1 GHz). The case n = 1.0 corresponds to a pure far field propagation, that may be criticized thinking that ground reflection is always present (although skin effect is negligible).

Table 1. Subdivision in frequency sub-ranges and advised sweep time values of EN 50121-3-1.

Interval	Subrange	Span	RBW	Sweep Time
A1	9–59 kHz	50 kHz	1 kHz	300 ms
A2	50–150 kHz	150 kHz	1 kHz	300 ms
B1	0.15–1.15 MHz	1 MHz	9/10 kHz	37 ms
B2	1–11 MHz	10 MHz	9/10 kHz	370 ms
B3	10–20 MHz	10 MHz	9/10 kHz	370 ms
B4	20–30 MHz	10 MHz	9/10 kHz	370 ms
C	30–230 MHz	200 MHz	100/120 kHz	42 ms
D1	200–500 MHz	300 MHz	100/120 kHz	63 ms
D2	500–1000 MHz	500 MHz	100/120 kHz	100 ms

In addition, Open Area Test Site equations in CISPR standards (considered by EN 50121 as a reference) are mostly based indeed on the assumption of flat, perfect ground. The measured field intensity always results from composition of direct and reflected rays, and the relative phase relationship and resulting overall rms at one frequency depends on the geometry and reflective characteristics of surface, including scattering. It is thus clear that the determination of the n values has underlying assumptions that in the EN 50121 are not made explicit. Given the range and variety of site conditions, such correction should be used wisely and moderately. Last, for viaduct sections measurements can be taken using a scissor-lift or other means to prop up the antenna set at the viaduct height: no ground reflection occurs and n values may be inapplicable.

Mapping of field variability for a better description of E-field intensity distribution is a good approach, but may be achieved at the expense of longer test time (see e.g., method RE102 of MIL-STD-461 [28]), where P equally spaced measurement points are deployed close to the source). This proposal finds its ground observing that many of the potential victims reviewed in the Introduction are located within the railway system

and that extrapolation to shorter distance occurs often in the reactive field region, with variable coupling between source and victim [14] and a poorly defined path loss exponent, especially for H-field components. The n values are defined for E-field only and vary significantly between 0.15 and 1.6 MHz, besides the fact that they were never defined between 0.009 and 0.15 MHz (even in the older 2000 and 2006 versions).

2.4. Detectors and Resolution Bandwidth (RBW)

Quasi-Peak (QP) and Average detectors are judged as obsolete for EMC purposes [18], as they weigh intensity and repetition rate of disturbance in a frequency range and with dynamics suitable for old analog communication systems. With the transient nature of emissions and the objective of assessing worst-case emissions in a safety perspective, the suitable detector is the Peak detector, without averaging or video filter. For stationary tests, in any case, the EN 50121-3-1 requires the use of a QP detector that agrees with CISPR standards [49], but does not allow a direct comparison with the results of the dynamic tests (where the Peak detector is used), as confirmed by Section A.2 of the EN 50121-2 (2015) itself. EMI (Electromagnetic Interference) receiver detectors have different responses and spot out different characteristics of the Intermediate Frequency (IF) output they process (see Figure 2 for graphical illustration). The signal fed to these detectors is the copy of the input signal after frequency translation to IF frequency and band limitation by application of the *RBW* band-pass IF filter [50]. In general, there is no straightforward and reliable rule to correct detector output in post-processing to recover the output that would have been obtained with another detector. The reason is that the operation of detectors depends on the IF signal dynamics and on the ordered sequence of signal variations, that belongs to the time domain and is lost after they are scanned in frequency domain and processed by a specific detector. Modern equipment is able to process IF output with a parallel application of available detectors. CISPR 12 [51] for automotive applications questionably establishes a fixed 20 dB conversion factor between Peak and Quasi-Peak detectors.

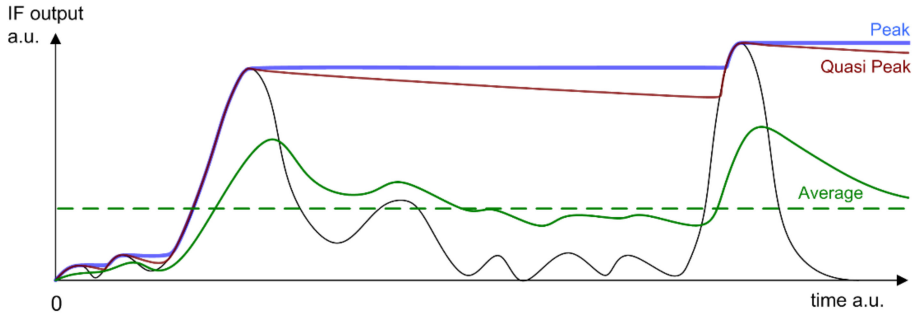

Figure 2. Sketch of detector operating principle on an ideal IF (Intermediate Filter) output, i.e., band-passed portion of the incoming signal: peak (blue), quasi peak (brown), average (green); for the average detector both the time varying trace tracking instantaneous average value and the conventional mean value at the end of the dwell time are shown—solid and dashed, respectively. Time and amplitude in arbitrary units (a.u.).

CISPR standards focus implicitly on EMC of small–medium size products, and are not concerned with the significant extension of the EUT, the Equipment Under Test (as similarly for large-power converters and drives [47,48]) and the dynamics of current collection.

RBW values are taken from CISPR 16 for the EN 50121, whereas UMTA rely on MIL-STD-461: 200 Hz (for the 9–150 kHz interval [16–19], optionally increased to 1 kHz for a sweep speed exigency), then 9 kHz up to 30 MHz and 120 kHz above it for EN 50121, and 10 and 100 kHz for UMTA [24].

There is no generally applicable rule for equivalence of measured field intensity for different RBWs [50,52]: square root of *RBW* ratio applies for incoherent noise with a flat power spectral density; *RBW* ratio is applicable to coherent signals, as shown in (2) for

voltage signals in linear form (in dB there will be a multiplying factor of 10 and 20 on the left and right k term, respectively). This is discussed further in Section 4.1.

$$k_{\mathrm{RBW,incoh}} = \sqrt{\frac{RBW_1}{RBW_2}} \quad k_{\mathrm{RBW,coh}} = \frac{RBW_1}{RBW_2} \tag{2}$$

2.5. Antennas and Antenna Orientation

Standards agree on the frequency-domain method, instrumentation (spectrum analyzer or EMI receiver and set of antennas) and main settings. There are also some differences, such as antenna types and orientation, summarized in the drawing of Figure 3. Antennas are identified by means of a simplified sketch with clear meaning: loop, biconical, log-periodic, and rod antenna.

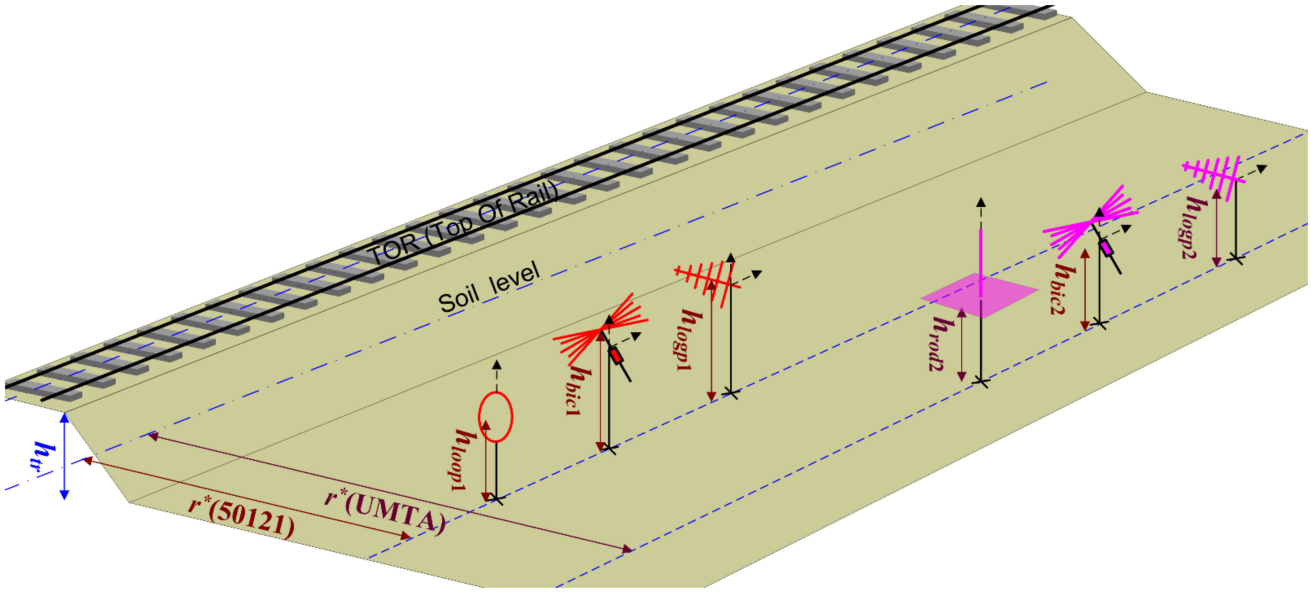

Figure 3. Sketch of antenna orientations as per EN 50121 (red) and Urban Mass Transport Association (UMTA) (pink): h_{loop1} = 1.5–2.5 m, h_{bic1} = 2.5–3.5 m, h_{logp1} = 2.5–3.5 m, and h_{rod2} = h_{bic2} = h_{logp2} = 2.0 m; orientation indicated by arrows.

Such antennas are the most common types, that in some cases we may say are the only ones allowed: strict interpretation, in fact—in particular for what concerns the EN 50121—would not allow the use of other types of antennas. Small antennas obviously are handy and allow measurements next to potential victims, but have lower directivity, thus increasing background noise (that includes the input noise of the measuring instrument). Large antennas, however, besides having logistical problems, might have a significant coupling with conductive parts and ground, as it is explained in [53] for the biconical antenna when changing orientation between horizontal and vertical for standard height above ground (2.5–3.5 m). A small antenna at the standard height above ground is immune from such undesirable coupling.

The update of listed antennas would allow measuring both polarizations at the same time without requiring a change of orientation (e.g., by means of a helical antenna or a large horn). The contemporary use of more than one antenna allows exploiting parallel recording, e.g., with synced spectrum analyzers or a high-speed oscilloscope: this not only gives a better representation of the time–frequency–space distribution of electromagnetic phenomena, but also allows reducing test times and the number of test runs.

Regarding orientation (also named antenna "polarization"), the EN 50121 requires both polarizations for E-field; the H-field loop instead must stand vertical parallel to the line. UMTA covers only E-field measurements and requires vertical polarization below 30 MHz,

both polarizations for 30–200 MHz, and only horizontal for 200–400 MHz, justifying it with the polarization of AM and FM radio signals at that time.

For height above ground and with respect to the railway system reference (TOR, Top Of Rail) there are different prescriptions; TOR is located in general at height h_{TOR} almost 0 and up to about 1 m above ground level (excluding cut and cover sections where measurements cannot be carried out).

- The EN 50121 prescribes three ranges of height values for each antenna that is indicated for a specific frequency range: range B (0.15–30 MHz) is measured with a loop antenna, whose center is placed with h_{loop} = 1.0–2.0 m measured with respect to TOR; range C (30–300 MHz) is measured with a biconical antenna, whose center is placed with h_{loop} = 2.5–3.5 m above TOR; and range D (230–1000 MHz) is measured with a log-periodic antenna, whose center is placed with h_{loop} = 2.5–3.5 m above TOR. It is remarked that 300 MHz is not a common upper frequency range for biconical antennas, that usually operate up to 200–230 MHz. Sweep time specifications in EN 50121-3-1 report instead 230 MHz as the limit between range C and D.
- The UMTA prescribes antennas in line with the MIL STD 461 and ANSI C63.4, placed at a height of 2 m above ground. Limits of new contractual specifications extend to 6 GHz and beyond (as shown in Figure 1): without an explicit indication of antennas to use, one can rely on the mentioned MIL STD 461.

E-field polarization and its coupling to the victim antenna is analyzed quite comprehensively in [14] for the specific case of electromagnetic emissions from the electric arc, to conclude that arc orientation (including the effect of speed and wind), as well as the staggering of the catenary, have a significant effect on the estimated coupling coefficient to the receiving antenna.

The observed variability of results between numeric simulations and scaled physical model is about −45 to −49 dB for inclined arc length ranging between 30 and 90 mm. Variability is only −45 to −44 dB for a wide range of staggering values (from 0 to 30 cm measured from the catenary axis) and it is between −50 and −44 dB for vertical catenary oscillations with gap of 10 to 90 mm (similarly, if the gap is created by pantograph folding rather than catenary rising). The power received by the GSM-R antenna with a *RBW* = 300 kHz is −50/−56 dBm at a distance of 19 m. Compared to [11], where at 30 m about −90 dBm over 200 kHz bandwidth at 900 MHz are measured, this power level is too large, even considering a correction of 4 dB for the ratio of distance and 1.76 dB for the ratio of *RBW* (see (1) and (2)). Practically speaking, GSM-R receiver sensitivity is about −85/−90 dBm for various transmission speeds and with some margin (pointed out in [11] and defined by the standards applicable to GSM-R [54]). The electric arc power indicated in [14] would made impossible any GSM-R transmission at more than 300 m or so, whereas the lower power level in [14] matches the frame error rate observed in [10,11].

2.6. Synthesis and Highlights

(2.1) Correction at distances other than 10 m is unreliable: one set of coefficient values for the path loss equation that is incomplete and influenced by ground (image current and reflections). Measurement distance as close as possible to 10 m is advisable.

(2.2) Comparison between limits of EN 50121 and UMTA/US Contracts shows wide differences, with the former far more permissive, although the susceptibility of victim systems around is in principle the same.

(2.3) The Peak detector must be preferred for frequency-domain measurements, instead of Quasi Peak and Average detectors, that obliterate signal dynamics. Sweep time must be correspondingly fast, as it will be discussed in Section 4.2.

(2.4) Use of smaller antennas, beyond the EN 50121 listed ones, would allow the evaluation of e.m. field emissions with a reduced influence of the ground and closer to the victims.

3. Operating Conditions and Measurement Methods

After having considered the basic measurement setup of Section 2, we now focus on the dynamic scenario of the railway line traffic, the relevant operating conditions and suitable measurement methods to control variability and uncertainty.

3.1. Vehicle as Moving Source

The vehicle cannot be considered a point source, as sketched below in Figure 4 (see the source points S_1, S_2, and S_3) and if we observe that wavelength and distance are both comparable with its dimensions [47]. The catenary should also be considered as an effective radiation means, further extending the physical size of the source (see [43] for an estimate of the effective length of the radiating catenary at various frequencies in the MHz range, which approximately ranges in the hundreds meters). As result, while the vehicle passes in the measurement area, significant variations of the measured intensity may occur.

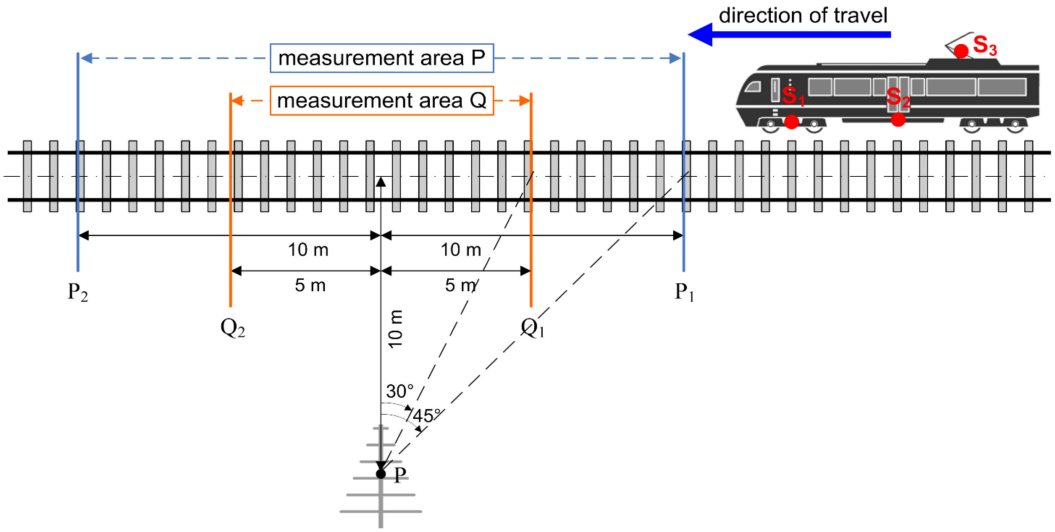

Figure 4. Sketch of the measurement area with passage points "1" and "2", where the instrument scan is to be started and stopped (in line with EN 50121-3-1): the measurement area defined by P_1 and P_2 is related to a ±45° angle, the area defined by Q_1 and Q_2 ±30°. The presence of the rolling stock should be accounted for the likely positions of the sources: S_1 (motor cables), S_2 (static power converters), and S_3 (pantograph).

For EN 50121-3-1 frequency sweeps are made with the vehicle passing through the measurement area, but for line emissions (EN 50121-2) measurements are performed also for vehicle positions relatively far from the antenna. Required dynamic conditions are different for EN 50121-2 and EN 50121-3-1: the former requires a faster speed, includes braking, but acceleration is not mentioned explicitly, focusing on cruising at rated speed.

The distance from the antenna changes as the vehicle moves through the measurement area (see Figure 4), with the minimum value r^* set by the prescribed antenna–track distance. This causes a slow modulation of the amplitude of spectrum components measured during one sweep or between successive sweeps. In far-field conditions (barely fulfilled at 30 MHz), E-field intensity E [V/m] is inversely proportional to distance r [m]:

$$E(r) = \frac{E_0}{r}\ E^* = E(r*)\ \frac{\delta E}{E} = \frac{E^* - E(r)}{E^*} = 1 - \frac{r*}{r} \tag{3}$$

The –1 and –3 dB points correspond to a distance increase of 12 and 41%, so to angles of 30° and 45°, that define the measurement area between the intercepts of points P_1–P_2 or Q_1–Q_2: the sweep starts when the vehicle passes past point "1" (P_1 or Q_1 for measurement areas P and Q, respectively) with the scan rate adjusted to finish approximately when the vehicle leaves past point "2" (P_2 or Q_2).

Various distances r^* are generally allowed by EN 50121 standards, indicating a conversion factor as discussed in Section 2.3, conversely, UMTA for broadband emission measurements (Method RE01A) indicates a distance of 30 m for antenna placement and no corrections. Such distance is surely preferable to extend the far field conditions to lower frequencies and alleviates the constraint on the measurement area extension, related to the amplitude modulation of the received signal while the vehicle is moving. Conversely, it is rarely practically viable, because the transversal extension of the right of way from the nearest track axis of a real line is not so wide. If such a wide area may be available at depots, then the conditions of traffic, speed, and line homogeneity are the impeding factors for the execution of compliant measurements. In addition, the signal-to-noise ratio at 30 m is at least 9.55 dB smaller accounting for a far-field path loss (exponent equal to unity). It is instead larger, if the nature of the correction factor in Section 2.3 is considered with a 15.7 to 17.2 dB reduction, resulting from the application of the two correction exponents of 1.65 and 1.8.

3.2. Traffic and Line Conditions and Train Composition

Environmental conditions are considered and discussed in [23]. For line measurements the verification of the presence of "physically-remote, but electrically-near" vehicles required in EN 50121-2 (2006) is now in the 2015 version, Section 5.4.3, are considered an insignificant factor. Nevertheless, Section 5.1.2 still requires measuring emissions "for a sufficient duration before and after the vehicle passage", since emissions may be higher at some low frequencies when the vehicle is a long distance away (emissions can be recognized in practice above the background noise for up to 1 km, especially those in the tens to hundreds kHz). Whether this change is paired with the removal of the A interval 9–150 kHz is not clear, although Section A.9.3 hints in this sense.

Substation loading and the number of trains in the supply section is a pre-condition removed in 2015, implying that tests are meaningful with just one vehicle and one substation loaded at only 10% or less. We can still find, however, in the EN 50121-2, Section 5.1.3, a statement saying that railway substations' load can change in a short time and that emission is related to load. The requirement then is only to annotate the actual substation loading during emission tests, besides that the complication of accessing values inside the substation (e.g., by accessing the logging of power metering devices or by direct measurement with all issues related to electrical safety and permit of access), raises a concern about loose specification of test conditions.

For the train and its composition EN 50121-2, Section A.10, acknowledges that coupled vehicles may cause higher emissions, but no minimum test configurations are identified:

- Coupled vehicles can increase measured emissions as the sum of the contributing terms of two or more units, although attenuation and phase rotation for the different distances should be considered. For this a correction coefficient may be devised, considering the direct emission from the past and next vehicles adjacent to the one passing in front of the antenna. Using the principle of (1), the E-field from an adjacent unit of 18- and 24-m length as received at the measuring antenna 10 m from the track would contribute -6.3 and -8.3 dB, respectively, in far field conditions. This is a figure absolutely comparable to the -6 dB criterion used to judge background noise components as excessive.
- Usually coupled vehicles and EMUs are not equipped with more than one pantograph or do not travel with more than one pantograph raised up, in such case the conducted emissions are injected into the catenary at the same point, but they are of course the sum of all contributions.
- The train line is longer and roof high-voltage cable connecting the pantographs contributes additional capacitance, affecting catenary resonance.

Based on the points above we may doubt whether the so-obtained measured data are reproducible and represent real emissions, and in particular worst-case emissions.

3.3. Stationary Conditions and Background Noise

Measurement in various stationary conditions is useful to discriminate sources of emissions, although this is not strictly required by all standards: the EN 50121-3-1 requires measurements in stationary condition (using QP detector) and indicates background noise measurements as advisable. However, the effect of the loco circuits loading the line when the pantograph is up and the emissions of auxiliaries are not mentioned.

A complete sequence of background and stationary conditions may be defined:

1. Background condition: no vehicle in the measurement area.
2. Background with locomotive parked in the measurement area in front of the antenna, pantograph down and all onboard apparatus off.
3. Locomotive parked in front of antenna, pantograph down, but auxiliaries fed by onboard battery and switched on.
4. Same as condition 3, but pantograph up touching the contact line.
5. Locomotive in traction mode, accelerating in front of the antenna with 1/3 of effort (EN 50121-3-1).
6. Locomotive in braking mode, braking in front of the antenna with 1/3 of effort (EN 50121-3-1).

There is a difference between conditions 1 and 2, corresponding to the dark and light grey curves of Figure 5, where the loco body in the measurement area has some influence, possibly capacitively loading the catenary or less likely causing reflections.

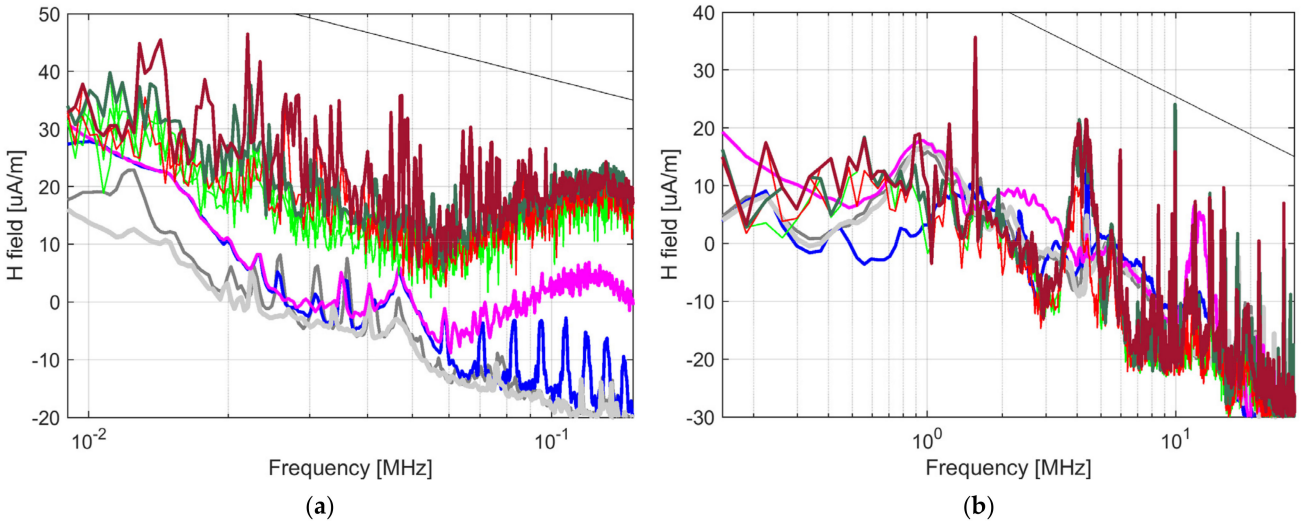

(**a**) (**b**)

Figure 5. H–field emissions of a DC locomotive: (**a**) horizontal and (**b**) vertical loop 9–150 kHz, *RBW* = 200 Hz. Operating conditions: background without loco (light grey), background with loco off and pantograph down (dark grey), auxiliaries on (blue), auxiliaries on and pantograph up (magenta), tractioning (green, dark thick red is for the envelope of maxima), and braking (red, dark thick red is for the envelope of maxima).

The harmonic peaks visible in the blue curve of Figure 5a (condition 3: aux on, pantograph down) indicate a direct emission from the locomotive body. The raised-pantograph condition (magenta curve) sees a higher field intensity at higher frequency (above 40 kHz, starting to show a line resonance at about 130 kHz), as the contact line increases the efficiency of emissions, masking the periodic pattern of the blue curve (with apparent frequency separation of about 12 kHz). The peak located slightly above 30 kHz in Figure 5a may appear not to meet the observed frequency separation of 12 kHz: in reality, it is located following a 6 kHz separation, suggesting that it is the only singly-spaced peak of an otherwise series of peaks located at twice the switching frequency of a power converter. Traction and braking test results have 2–3 traces each: the envelope of maxima in bold shows slightly larger emissions for the braking condition.

In the 0.15–30 MHz interval of Figure 5b there are narrowband components due to radio transmissions, a significant amount of emissions from auxiliaries (the magenta curve) and a broad peak at about 4.5 MHz. The latter can be distinguished from a resonance after a step-by-step reasoning: the observed overall bandwidth of the max-hold brown curve is about 700 kHz, but the peak shape is in reality made of two major peaks with less than half bandwidth each (about 300 kHz). The fractional width compared to the central frequency is about 10%, that is what is normally assumed for line resonances as shown later in Section 3.5, occurring at a frequency smaller by two orders of magnitude. Thus, considering line losses and skin effect (proportional to the square root of frequency) a ten-fold larger bandwidth should occur in the present case if it were a line resonance. Then, finally, as a confirmation, separate measurements excluding the main auxiliary converter demonstrated the source of this emission, as a common-mode resonance along the converter cabinet and locomotive chassis.

Measuring background noise allows spotting out external sources (EN 50121-2, Section 5.1.12), and the 2015 version sets a 6 dB criterion with respect to limits, with frequency points excluded when closer than that. It should be noted that a max-hold scan of the background noise risks excluding from subsequent measurements more points than a cautious statistical assessment, negatively affecting the tests by reducing the number of frequency points subject to evaluation. A complete and accurate statistical assessment of background noise is preferable, but requires repeated measurements, against the common policy of carrying out the tests in the shortest time possible.

Repeated measurements and assessment of data dispersion [55,56] are exemplified in Figure 6, where individual sweeps are overlapped, with average and +1σ profiles in bold. The frequency axis is cut at 90 MHz to keep the figure compact: beyond this point FM broadcast, radio amateur and television are the only significant sources. This is a consideration based on the known behavior of emissions from large-power converters and the higher attenuation that characterizes the rolling stock enclosure and the catenary, and is confirmed by experience.

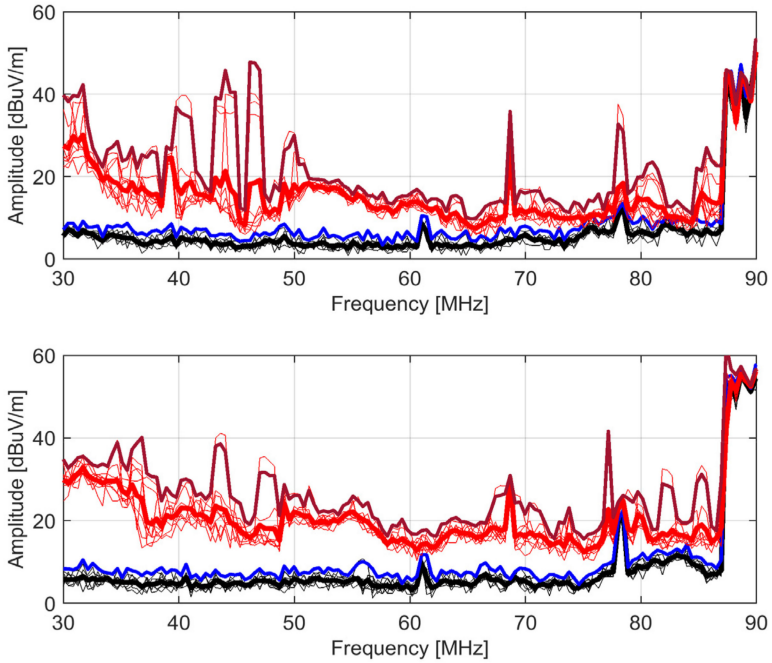

Figure 6. E-field intensity measured for qualification of a trolley bus (frequency interval limited to 30 to 90 MHz for displaying purpose): background (data black, mean thick black, +1σ profile blue) and emissions in simulated run (data red, mean thick red, +1σ profile brown). Note: "simulated run" refers to the trolley bus unit propped up on suspending tripods and wheels running free.

The background is particularly quiet with only two components at 61 and 78 MHz, then masked by vehicle emissions during tests. When the +1σ graphically sits as an upper bound on the set of curves, it means that the values are not too dispersed. It is on the contrary commonplace that measurement results are characterized by outliers, for both emissions (when transients are captured as scattered peaks at one or few frequency bin) and external sources (radio transmissions that background measurements could not fully characterize. This last point can be seen for the components at 69 and 78 MHz, that were not "captured" by the background noise measurements (six traces, peak detector, each max hold lasting 20 s), but occurred during the emission measurements (another 10 traces, peak detector) carried out about 15 min later. There are in fact several radio sources with a significantly intermittent behavior that fail to be adequately characterized by few measurements carried out over time intervals of some minutes and by the assessment carried out only by standard deviation evaluation.

Another important point is the relevance of transient emissions and if they should be included or not. The EN 50121-2 speaks of major transients caused by circuit breakers and similar devices to be excluded, but the transients considered here are the common on-off cycles of auxiliary converters, fans, compressors, etc. that should be well considered part of the normal operating conditions.

3.4. Vehicle Operation, Driving Style, and Synchronization

Tests are arranged to reproduce conditions of traction, cruising and braking. The EN 50121-3-1 requires that traction and braking are applied at one third of the maximum intensity when the vehicle is in the measurement area. If the vehicle is capable of electric braking, tests as per EN 50121-2 must use a braking intensity of at least 80% of the rated maximum value [16,17]. It is worth observing that empty vehicles and shorter trains must be ballasted to ensure adhesion and stability. In general, a light vehicle would decelerate too fast during braking with a short stopping distance, deceleration lasting less than a complete scan. UMTA and US specs have no requirements for traction or braking effort, nor for cruise speed.

A carefully synchronized measurement site and setup is not, however, the best solution in terms of representativeness and significance of measured emissions, although repeatability and reproducibility would be maximized (see Section 4.4). Having sweeps and vehicle passage tightly synchronized affects the location of spectrum peaks caused by transients, captured during the sweep itself: the energy content of an impulsive transient is spread over a large frequency interval with an approximately flat spectrum profile and is captured with similar intensity at different frequency points by the concomitant frequency sweep. The consequence is the impression of a line resonance or a specific narrowband vehicle emission attributed to a local increase of the swept profile: only careful de-synchronization of the sweep with respect to the start of traction or braking phase and the use of multiple scans and test runs allow verifying if such observed peak undergoes a frequency shift. This is an example of ambiguities of the frequency domain approach, whose strong side remains the signal-to-noise ratio and dynamic range.

The profile and shape of measured emissions are significantly affected by the driving style: the use of max-hold setting (see Figure 7) or statistical methods is advisable, provided that collection of sweeps in one train passage and the number of repeated passages are sufficient. This problem is considered in Section 4.4, where considerations related to confidence interval, repeatability, and uncertainty are proposed. An untimely synchronization is a source of systematic error that no statistical technique can remedy.

Figure 7 is an example of dependency of the spectrum shape on operating conditions and the relative position between the antenna and the point where tractioning or braking begins (see Figure 4 and Section 3.1). Measurements were taken at the two ends of a platform where metro trains in normal service coast and decelerate to stop (passing in front of pos. 1) and then depart with a traction phase (passing past pos. 2). As expected, the largest emissions occur for traction and braking depending on position, whereas at

higher frequency in general traction has the highest profile. The hump at 35 kHz is a line resonance visible at both positions, but in traction conditions it is almost hidden by the spectrum components.

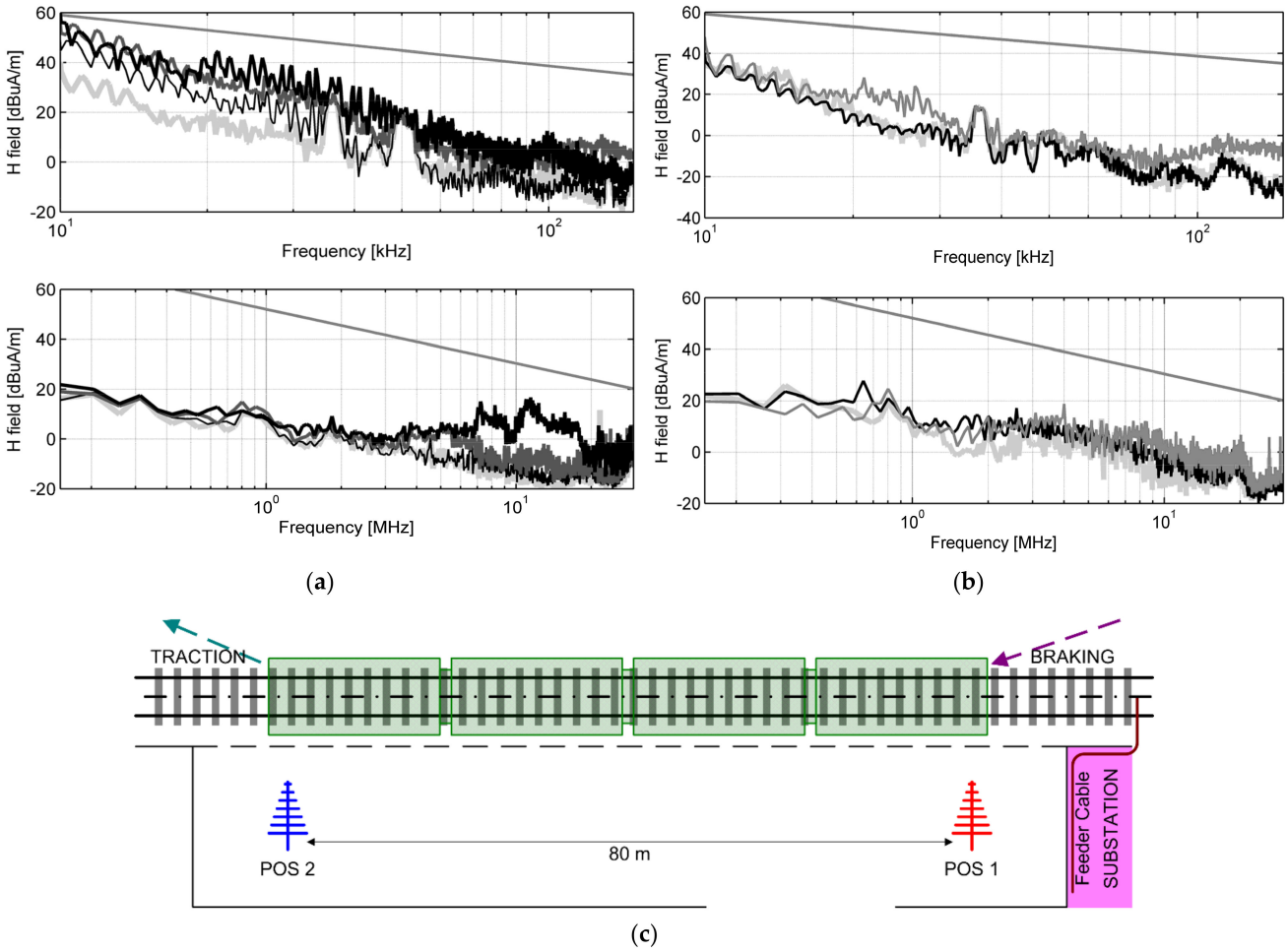

Figure 7. Measurement of train in commercial service: (**a**) pos. 2 (left platform end) and (**b**) pos. 1 (left platform end); distance between pos. 1 and 2 about 80 m. Operating conditions: background (light grey), braking (dark grey), coasting (thin black), and traction (thick black). (**c**) sketch of platform, measurement positions, braking/traction phase, and feeder cable from substation to catenary.

The intensity of emissions at pos. 2 is higher, as a shunting capacitive effect of positive feeder cables occurred at pos. 1 (visible in Figure 7c as the brown cable connecting to the catenary): comparing braking curves available at both positions, besides the effect of the distance, the attenuation is about 13–15 dB. The high-frequency emissions at both positions are mostly direct from the train body passing in front of the antenna, with the highest values for braking at pos. 1 and for traction at pos. 2.

3.5. Line Resonances

Propagation and radiation of emissions along the line are variable and depend on resonances, with the line impedance varying significantly. Examples of resonances can be seen in Figures 7 and 8 and they are particularly evident for up to a few hundred kHz (see also the comment on the unlike resonance at 4.5 MHz in Figure 5).

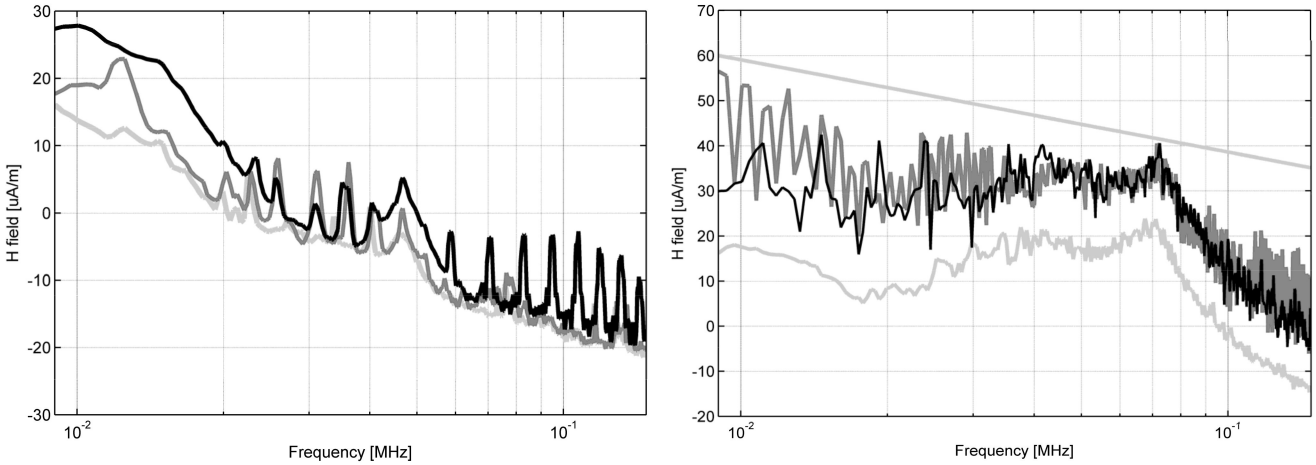

(**a**) (**b**)

Figure 8. Line resonance and interaction with rolling stock (same test track and location with two different locomotives): (**a**) no vehicle in the measurement area (light gray), auxiliaries on with pantograph down (gray) and up (black); (**b**) background (light grey), braking (dark gray). and acceleration (black). Shift of line resonance from (**a**) 47 kHz to (**b**) 72 kHz.

In principle, line resonant behavior in a broad sense (both resonances and anti-resonances) can be described by the following expressions, where the considered traction line stretch is between two sharp discontinuities, such as two Traction Power Stations. Besides major discontinuities (e.g., a neutral or phase separation section, a junction or feeder cable connection at substation), minor discontinuities can create secondary resonant behaviors (e.g., joining between open and tunnel sections).

$$Z = Z_c \frac{\tan \mathrm{h}(\gamma x L) \tan \mathrm{h}[\gamma(1-x)L]}{\tan \mathrm{h}(\gamma x L) + \tan \mathrm{h}[\gamma(1-x)L]} \quad \gamma = \sqrt{(r + j\omega l)(g + j\omega c)} \tag{4}$$

$$\omega_r(k, L) = \frac{k\pi v_0}{L} \quad \omega_a(k, x, L) = \frac{k\pi v_0}{x} \text{ and } \frac{k\pi v_0}{(L-x)} \tag{5}$$

where v_0 is the wave speed, L is the line length, x the position of the train, α and β are the real and imaginary part of the propagation constant (named attenuation and phase constant) [57]. The parameters r, l, g, and c are the per-unit-length resistance, inductance, conductance, and capacitance of the line [58] (g of catenary conductors can be neglected).

A traction line in resonant conditions has some peculiar behavior for what concerns electromagnetic emissions (see e.g., [38,43] for two related mathematical formulations):

- Some components are amplified increasing the impact on equipment nearby and the chance of interference. At anti-resonance the intensity of current components increases and, as a consequence, of H-field emissions. Conversely, E-field emissions increase in resonance conditions. Electromagnetic field emissions are a space–time concept [38], for which they are distributed along the frequency axis and the longitudinal position, but they depend also on the antenna height above ground, as shown later in Figure 9 (see behavior around 700 kHz).
- Early announcement of train arrival at the measurement site with its emissions well visible when the train is still far away. This is quantitatively shown in [43], Figure 10, where the calculated H-field at 30 m from track attenuates less than 10 dB in the first 2000 m up to about 0.5 MHz, and then more than 20 dB at 1 MHz and above. The emissions observed at line resonance and in the low frequency range (see e.g., Figure 5) are then clearly visible up to about 2 km of distance.
- Field intensity at resonance may be highly variable depending on antenna height and orientation. In particular, the reason is that the field source is in high impedance with the appearance of a longitudinal electric field component that is usually negligible in

low to medium impedance conditions (experimental evidence of the variability and field distribution is shown in Figure 9 for a third rail system [59]).

- Resonances slightly change with train position, although theoretically resonances of the line impedance do not [57]: the reason is that the magnetic components are strongly related to the line current, increasing at line anti-resonances, known to linearly depend on train position [57]. The total measured electromagnetic field is a mix of several modes of emissions in the reactive field region, related to both current flow and longitudinal voltage drop.
- Resonances and propagation characteristics are determined by the combination of line r, l, and c parameters, with different degrees of accuracy, depending on the estimate methods. Inductance l is a sufficiently stable parameter with a negligible contribution from internal inductance of running rails at these frequencies [60,61]. Capacitance c may be in principle determined with great accuracy [45,58], but is affected by elements other than line conductors (connected cables and transformers, adjacent lines, and rolling stock enclosure). Losses due to skin effect [43,61] and damping provided by connected elements should be added to the pure ohmic value of r, derived from cross section and conductivity information.

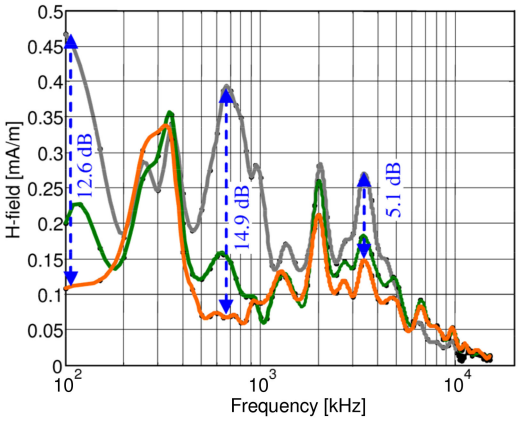

Figure 9. H-field intensity measured to qualify a short test track (metro line with third rail supply) [59]: three distances, d = 4 m (gray), 6 m (green), and 10 m (orange); height above ground of the base of loop antenna h = 0.25 m. The spread between curves in dB at the three major frequency points is indicated in blue.

In general, emissions peaks and line resonances may be observed with different frequency width. Emission peaks are narrowband and the perceived width may be influenced by the used *RBW* larger than their frequency spread (the δf at the -3 dB points in all cases amount to $\leq$1% the central frequency f_c, such as in Figure 5a). Line resonances are broader with a smaller factor of merit due to skin effect and line losses (see the broad peak at about 47 kHz in Figure 5a for grey, blue, and magenta curves, where $\delta f / f_c$ amounts to about 10%). They are also influenced by the internal train circuits loading the line (as shown in Figure 8, the main resonance of the same test line considered in Figure 5a moves from 47 to 72 kHz).

The question also arises if resonances must be excluded with a well-devised setup, as advised in EN 50121, so to optimize repeatability and uncertainty, or must be duly considered, as the faithful representation of (nearly) worst-case emissions. The need to identify line resonances is in Section 5.1.9 and B.10 of EN 50121-2 [16] and Section 6.3.1 of EN 50121-3-1: "if line resonance exists, this should be noted in the test report", that to this aim, however, a significant number of traces should be acquired is not remarked in the standard. On the other hand, minimization of uncertainty is a general exigency of the EN 50121 standards and is discussed later in Section 4.4. So, it appears that handling of line resonances for measurement purposes is subject for now to two opposite requisites, without a clear indication on suitable methods. Initial identification of line resonances can

be carried out exploiting stationary conditions with pantograph up (loading the line) and auxiliaries on (exciting the line), as shown in Figures 5a and 8.

3.6. Synthesis and Highlights

(3.1) The vehicle is a moving source and measurement distance and recorded test run should account for variability of distance from the antenna and unavoidable modulation of the received amplitude of the electromagnetic field.

(3.2) Background noise and extraneous emissions can be identified if a thorough characterization is carried out that balances statistical evaluation with a more straightforward max-hold scan that would unavoidably overestimate background noise—biasing favorably the compliance assessment of the rolling stock.

(3.3) A sequence of measurements is proposed for vehicle characterization, that accounts for the effect as a passive load by connecting to the line with the raised pantograph, as well as the contribution of the auxiliaries, besides the well-known conditions of tractioning and braking.

(3.4) The traction line has a complex resonant behavior, enhancing magnetic and electric field emissions by anti-resonances and resonances of the line impedance, respectively. As a phenomenon distributed in time and space it varies with frequency and longitudinal position, but also height above ground of the measuring antenna. The overall resonant behavior is also influenced by the rolling stock itself.

(3.5) Resonances are part of the normal operation of the line and of the line–vehicle interaction and should be included in the assessment of emissions and not considered as data aberrations.

(3.6) Transients, similarly, if not caused by singular characteristics and defects of the line, but related to normal operation, should be measured with suitable instrumentation settings (*RBW*, sweep time, and number of traces) and statistically evaluated. This aspect is further discussed in Section 4.

4. Instrument Settings and Spectral Characteristics

The instrumentation settings required by the standards and related assumptions are reviewed and commented, focusing on the impact on accuracy and uncertainty [56–58,62]. New techniques suitable for transient emissions and for digital communication systems susceptibility are also considered.

4.1. Limits and Broadband/Narrowband Assumption

EN 50121 and US specifications express limits differently: dBμV/m for the former, dBμV/m/MHz for the latter.

Signals may be classified as narrowband or broadband not by their very nature, but depending on the occupied spectrum relative to the *RBW* of the measuring instrument [52]. Converter emissions in differential mode contain harmonics of the converter switching pattern and some ringing and resonance effects, so that they are characterized by a line spectrum where components are narrowband. Conversely, common-mode byproducts that leak through parasitic elements have high-pass behavior, and, similarly, other transients such as electric arcs. for this reason, they are classified as broadband.

Broadband signals may be further divided into impulsive and random, observing the behavior with respect to the adopted *RBW*:

- impulsive signals are coherent and their spectrum components add their amplitude in phase: a 10-time increase of *RBW* results in a 10-time (20 dB) increase of the measured amplitude;
- random signals (e.g., noise) are incoherent and additive in power, not in amplitude, so the measured amplitude goes with the square root of *RBW*, or in other words for a 10-time increase of *RBW* the resulting increase of amplitude is 10 dB only.

Values can be expressed per MHz (frequency band normalization) when the signal may be assumed broadband and coherent. Narrowband components should not be expressed

normalized, to avoid giving the impression that with a different *RBW* value their amplitude would change. For impulsive signals (considered as a common example of the broadband category) normalization should be done more cautiously using the impulse bandwidth B_i and not *RBW*, with B_i ranging approximately between 1.2× and 2×*RBW*, depending on the type of IF filter [50,62].

RBW affects not only single spectrum components, but also groups of adjacent components. Repetitive impulsive signals (e.g., commutation transients and electric arc) result in a line spectrum and different amplitude readouts depending on the *RBW* value compared to their repetition frequency. Larger *RBW* values will collect more spectrum lines, resulting in increased amplitude. Switching in modern converters occurs at some kHz or tens of kHz, in correspondence with the mostly used *RBW* values, thus maximizing the sensitivity of the results to this phenomenon.

In summation, results may differ depending on the type of signal (transient, sinusoidal tone, and modulated or not) and its repetition rate, and a unique narrowband/broadband conversion factor is hard to find.

4.2. Sweep Time (ST) and Resolution Bandwidth (RBW)

First of all, the rolling stock as a moving source requires an *ST* fast enough for operating conditions and distance from the antenna when moving through the measurement area to be approximately constant during a sweep (Section 3.1). A faster *ST* value will better capture transient emissions [52]. A minimum bound is given by the selected *RBW* (that sets the IF filter transient response) and the number of points N_{tr} making a trace: the dwell time *DT* at each reading of the IF filter output multiplied by N_{tr} gives the total $ST = N_{tr}\ DT$.

Table 1 shows the subdivision of frequency intervals into sub-ranges done in EN 50121-3-1 to ensure that the maximum *ST* requirement is achieved. Then *ST* requirements are compared in Table 2 for EN 50121-2, EN 50121-3-1, and MIL STD 461.

Table 2. Sweep time values (EN 50121-2, EN 50121-3-1, and MIL STD 461G).

Standards	Frequency Intervals	
	0.15–30 MHz	**30–1000 MHz**
EN 50121-2, Table 2	300 ms/60 km/h 60 ms/300 km/h	300 ms/60 km/h 60 ms/300 km/h
EN 50121-3-1, Table B.1	37 ms/MHz	0.2 ms/MHz
MIL STD 461G, Table II	1.5 s/MHz	0.15 s/MHz

EN 50121 requires faster *ST* than MIL STD 461 by a factor of 10 to 50. It is peculiar that EN 50121-2 has faster *ST* than EN 50121-3-1, simply because the test speed in the latter is lower, remembering that for EN 50121-3-1 the sweep must scan the whole passage in front of the antenna (see Section 3.1). In order to test all relevant operating modes and considering modern faster trains, EN 50121-3-1 should give prescriptions for higher test speeds. In this case, *ST* values should be further reduced, increasing correspondingly the number of sub-intervals to comply with the 60 to 300 ms overall requirement or definitely using time-domain equipment [63–65], achieving multiple measurements during one train passage.

There is one prescription, however, in the EN 50121-2, Section A.3 that may cause some confusion: a 50 ms time window is recommended at each selected frequency, quite slow compared to the *ST* values in Tables 1 and 2. This is a leftover of the prescription of acquiring at least one AC fundamental half period for capturing electric arcs that in AC systems occur around zero crossing (in 16.7 Hz systems the half period is 30 ms).

As for *ST* constraints, spectrum analyzers operating in swept mode are burdened by the transient response of the IF filter that limits the minimum dwell time at each frequency bin: the classical formula for the sweep time shows inverse proportionality to the square of *RBW*.

$$ST = k_1 \frac{\text{span}}{RBW^2} \tag{6}$$

where k_1 is a factor that depends on the transient response and settling time of the IF filter and usually ranges between 1.5 and 3.

The most critical situation occurs at low *RBW* values that however are not of concern, except to extend the analysis to the 9–150 kHz frequency interval. Sweeping this interval at *RBW* = 200 Hz requires $k_1 \cdot 3.52$ s, using 50% overlap obviously increases *ST* to $k_1 \cdot 7.04$ s. Pushing the *RBW* to 1 kHz (allowed by the EN 50121-3-1) results in $k_1 \cdot 0.14$ s and $k_1 \cdot 0.28$ s, respectively. For the second 0.15–30 MHz interval, the sweep speed does not improve, as it requires $k_1 \cdot 0.37$ s without overlap; assigning a sensible value to k_1 (e.g., 2.5) and avoiding overlap, the resulting *ST* barely complies with EN 50121-3-1, but not with the EN 50121-2 (see Table 2). This is the reason for splitting such frequency interval in sub-ranges with smaller span.

Modern spectrum analyzers and signal analyzers work on time-domain signals and achieve the spectrum representation with an elaborated scheme based on Fast Fourier Transform, distinguishing between Real Time Spectrum Analyzers (RTSA) and non-RTSA, the latter processing only one signal window every *M*. With these machines the sweep time (named for uniformity) is:

$$ST = k_2 \frac{1}{RBW} \tag{7}$$

where k_2 is a factor that depends on processing implementation details and speed of calculation and data transfer, and *RBW* is in reality the bandwidth of one FFT bin, i.e., approximately the inverse of the time window length (if tapering windows are used, their characteristics may be absorbed in the k_2 coefficient [66,67]).

The left and right tails of a tapered window are affected by significant amplitude error (about 10% of the window length for each side, but depending on the used tapering window a more accurate assessment of its impact may be done, as in [68,69]). For this reason, some amount of overlap is always necessary to track accurately all signal components. It is easy to see that, provided that the FFT buffer is sufficient, *ST* values of some ms can be achieved with *RBW* = 1 kHz. The 0.15–30 MHz interval at a CISPR-compliant *RBW* = 9 kHz would be processed in about 40 µs. Lower *RBW* values down to e.g., 1 kHz are possible, but physical limitations of processing speed and transfer rate to memory keep the achievable performance in the order of a about ten millisecond.

4.3. Time Domain and Amplitude Probability Distribution

The largest share of emissions for assessment of interference to modern digital communications is of transient type, related to the electric arc emissions: the measurement method must cope with the short duration of each transient, separated from the adjacent ones by long intervals. Such peaks may be captured by frequency domain equipment set to max hold with a fast sweep or zero span mode: the arc time duration shown in [11], Figure 4 (namely up to about 30 ns) requires a minimum *RBW* of 10 MHz and the use of compensation for pulse desensitization ([50], Section 9.2.13). Pulse desensitization gives smaller amplitude readings at smaller *RBW* values, when a pulsed signal is subject to measurement: the desensitization factor can be expressed as $\alpha = 20 \log_{10}(\tau k B)$, where τ is the duration of the pulse, *B* the bandwidth, and *k* the shape factor. The impulse bandwidth *B* can be made correspond to *RBW* with some approximation: the value of *k* then weighs the type of filter, being 1 for a Gaussian filter, 1.5 for a rectangular one, and all of the others lying in between. Setting $\tau B = 0.1$ [50] is a good compromise for amplitude and frequency accuracy.

Information related to time distribution and repetition rate would be approximately preserved only in zero-span mode. Such information is quite important when it comes to assess interference with communications protocols that work on time slots shared between channels (combination of Time Division Multiple Access and Frequency Division Multiple Access, typical of GSM) and where the access to the channel is negotiated with an exchange of control data with tight timing (IEEE 802.11 and LTE protocols). The GSM-R tested in [11], Figure 10, was quite robust and the Bit Error Probability (BEP) linearly increased when

the repetition rate was increased. Considering the IEEE 802.11n tested in [2], keeping the intensity of the transient disturbance constant with no visible degradation, when the repetition interval reached 26 µs the channel was suddenly inaccessible for continuous detection of busy status. Modern transmission technologies imply a phase of negotiation and access to the channel, followed by a phase of transmission and quality control, all carried out with time multiplexing, using a variety of channel coding techniques.

Therefore, looking at the weakness of the swept frequency-domain method and achieving a better definition of the susceptibility of modern digital communication systems (DCSs), the Amplitude Probability Distribution (APD) method is being studied [69–73], e.g., in place of other types of detectors, such as the QP. The APD quantifies the amount of time that the measured envelope $r(t)$ of an interfering signal exceeds a given level [69], or, in other words, it is the complement to unity of the cumulative distribution function of the envelope. The APD is particularly well suited to quantify disturbance to a wide range of DCSs and resulting BEP.

APD can be measured using a spectrum analyzer with an envelope detector limiting the scan to the operating band of the radio system, but a time domain approach has more flexibility. The method to assess interference and impact on BEP for a wide class of digital coherent radio receivers was shown in [69], and it can be equivalently transferred to other coding and detection schemes. The APD is already included in CISPR 16-1-1 [49] for use above 1 GHz, but its application is lagging in [74] it is said that APD is listed as long-term work item in a future amendment of CISPR 32 [75].

It is remarked that APD gives information on the amplitude distribution, but fails to characterize the time distribution, e.g., in the case of repetitive pulses. A joint time–frequency transform can display the power spectrum distribution over time [11], so that some kind of periodicity can be captured, although evaluating long repetition intervals compared to pulse duration is unpractical. Yet, a more complete characterization is achieved if the time distribution of interfering pulses is considered too. In [72], the overall assessment is made in two steps, starting from an APD evaluation of the interference to a single code block (BLER), under the assumption that all bits of a block are equally affected (suitable assumption if Forward Error Correcting code and interleaving methods, such as turbo codes or low-density parity check codes, are used). Then, the repetition interval *RI* is compared to the code block duration and a comprehensive model is derived for the overall long-term BLER. Simulations with hardware-in-the-loop give values that for *RI* between 10% and 100% of block duration are quite similar to [11], Figure 10 thus is slightly pessimistic.

4.4. Uncertainty, Repeatability, and Statistical Significance

Reproducibility and uncertainty are scarcely covered, as only EN 50121 mentions it and a bit ambiguously: low reproducibility was invoked for the removal of the 9–150 kHz interval without further requisites and guidelines. Assessment of uncertainty is also limited to instrumental uncertainty with a reference to CISPR [49]. Reproducibility and uncertainty may be defined as follows:

- Reproducibility is the closeness of agreement between the results of measurements of the same measurand, carried out with the same method. It measures the agreement of results obtained in different scenarios (e.g., different test sessions or campaigns) using the same method [76], for which procedures must be clear and non-ambiguous and instrumentation must be well characterized.
- Uncertainty characterizes the dispersion of the values that could reasonably be attributed to the measurand [55]. If systematic error occurs, uncertainty must be evaluated after correction is applied. Incomplete information to define and apply the correction brings in a further term of uncertainty.

There are various and different elements that influence measurement error: first of all, instrumentation, its settings (e.g., *ST* and *RBW*), and measurement setup. The environment and background noise are another source of error. Lastly, operating conditions and their variability have a more complex influence, causing systematic and random errors. The

accuracy limit of EN 50121-2 (2006) was ±4 dB for instrumentation, with a reported repeatability of about 10 dB. Now, the 2015 version speaks of uncertainty and refers to CISPR 16-1-1 (instrumentation) and 16-1-4 (antennas and site uncertainty), excluding the normalized site attenuation from the uncertainty budget and justifying it simply with a reference to the "measurement method". As a matter of fact, any reference to repeatability and evaluation of data dispersion is lost, and uncertainty assessment is limited to instrumentation.

Reproducibility is influenced by clarity and completeness of procedures, so to ensure the same level of repeatability in different conditions (e.g., drivers, type of rolling stock, etc.) and by the removal of outliers and background noise, that might affect locally data dispersion.

Uncertainty should be evaluated in two ways: Type B method covers instrumentation uncertainty (the starting point for compliance to EN 50121), but a more general Type A approach (based on the assessment of data dispersion) allows evaluating repeatability, reproducibility, and statistical consistency of measurements [63]. To this aim, different time scales must be considered:

- short-term dispersion within the same tests session evaluates repeatability;
- repeatability may be assessed for a scenario with same instrumentation, setup and test track on a longer time interval (e.g., different test runs in different days);
- reproducibility is then evaluated by means of comparison of repeatability figures, calculated for different scenarios, characterized by different tests sites and setups, unavoidably combining the influence of both procedures and site characteristics.

The EN 50121 and UMTA standards do not indicate a minimum number of traces and test runs, so that in practice only one measurement is taken, claiming that a max-hold scan will provide a worst-case profile of emissions. As such, it was shown that this is not due to synchronization issues with traction/braking events (Section 3.4), influence of line resonances at some distances from track and longitudinal positions (Section 3.5), and observed dispersion of traces acquired in nominally identical conditions (Section 3.3).

In general, when assessing compliance to limits for products, the CISPR 11 [41], Annex H, prescribes a coefficient k_E that depends on the sample size and multiplies the estimated dispersion σ_{ref} of the sample of products:

$$X + k_E \sigma_{ref} \leq \text{Lim} \quad (8)$$

where X stands for the measured value of e.m. field after processing (see below), Lim is the limit value, and k_E and σ_{ref} may assume different meanings depending on the used approach.

The approaches proposed by the CISPR 11 are:

- General a priori margin: σ_{ref} is taken as 6 dB (based on CISPR 16-4-3) and k_E depends on the sample size n (k_E = 0.63, 0.41, 0.24, 0.12 for N = 3, 4, 5, 6, respectively). Since the standard speaks of a coverage factor of 2 in relation to the 6 dB figure, it implies that the assumed standard deviation of the measured data is 3 dB.
- Assessment based on the non-central t-distribution: σ_{ref} is estimated as the standard deviation and X is the mean of the measured values of the sample with sample size n prescribed to be between 5 and 12. k_E is set for an 80% confidence that 80% of the production (i.e., of all emissions from the rolling stock or line) is below the limit, so k_E = 2.04, 1.69, 1.52, 1.35, 1.30, 1.27, and 1.24 for n = 3, 4, 5, 6, 7, 8, 9, and 10, respectively.

Provided that the sample size (number of test runs n seen as realizations of the same system) is adequate and that data are preliminary screened to identify outliers, sample standard deviation and higher order moments can give an accurate estimate of repeatability and uncertainty (see the multiple traces in Figure 6, and the location of the mean and +1σ curves). The N value is a compromise between a tighter confidence interval and minimal test duration. Regarding the assumed standard deviation of 3 dB in CISPR 11, it is observed that real emissions are more dispersed, as previously commented: the

stated 10 dB repeatability of EN 50121 and frequent distance of 10 to 30 dB between mean and +1σ curves in Figure 6. Thus, a specific approach with suitable margins turns out to be necessary.

Furthermore, considering external intermittent sources, transient emissions and a variable system response (moving resonances), sample standard deviation, and criteria based only on amplitude might be insufficient or inappropriate in some cases. More robust techniques should be considered, such as algorithms that evaluate similarity between curves through details like shape, slope, etc., besides height and position of peaks, ensuring however an unambiguous relationship with the known quantitative criteria used so far by the standards.

4.5. Synthesis and Highlights

(4.1) Speed of scan, detailed spectrum representation, and adequate characterization of phenomena with different spectrum occupation are different exigencies that the selection of the *RBW* value tries to trade off. Values of 0.2–1 kHz, 9–10 kHz, and 100–120 kHz are a suitable compromise for frequency domain sweeps for the A, B, and C+D frequency intervals (in the CISPR sense, not different from the UMTA definitions). For interval A, 1 kHz is by far preferable and allowed by the EN 50121-3-1.

(4.2) Electromagnetic emissions are characterized by both narrowband and broadband phenomena, where the former are exemplified by switching harmonics, and the latter by electric arc and switching transients. Some are periodic phenomena (switching transients arranged as a pulse train) others are random (electric arcs), although repetitive to some extent. A unique conversion rule for the use of different Resolution Bandwidth values is not possible.

(4.3) For the measurement of purely transient phenomena (e.g., electric arc) a larger *RBW* value is advisable, in order to minimize the settling time of the IF filter. However, in such case real-time spectrum analyzers, or better time-domain acquisitions give better results, when followed by post-processing techniques yielding a time–frequency representation of the disturbance, suitable for assessment of interference to modern digital communications.

(4.4) Uncertainty is too simply limited to instrumental uncertainty in the two latest versions of the EN 50121 and not considered by US specifications. It was demonstrated that several factors are relevant to the uncertainty that should also be evaluated with a Type A approach, having identified and corrected systematic errors. Such factors are: site response, variability of emissions, variability of line response, transient events, driving style, external sources, and background noise.

(4.5) Such an approach to uncertainty would allow the evaluation of repeatability and reproducibility, establishing minimum requirements for site selection, beyond simple criteria based on distance from conductive elements and line discontinuities.

5. Conclusions

Standards used for the measurement of radiated emissions of electric transportation systems and rolling stock have been considered: EN 50121-2, EN 50121-3-1, and UMTA specifications (with some contractual specifications), the latter based mainly on MIL-STD-461G. The main factors affecting measurement results (in terms of spectrum distribution and variability) and the measurement uncertainty are many: instrumentation settings and setup, in particular to cope with a moving source that is extended in space. Line resonances and transient nature of emissions may not be clearly distinguished as they appear as peaks with various perceived bandwidths. Then, operating conditions, site response and issues of synchronization with train passage (e.g., driving style) are complex sources of uncertainty and also systematic errors. Some examples taken from past tests of railways, metros, and trolley buses have been analyzed and discussed, in order to identify suitable approaches and guidelines.

The discussion aimed at spotting out unclear or inconsistent points, including possibly inadequate or incomplete standard prescriptions, and then suggesting points to check and best practices. The latter have been synthesized at the end of each section for reader's ease.

High-level guidelines for accurate and reliable measurement of emissions may be synthesized as:

- consistent characterization of background noise: the first aspect is the characterization in terms of statistical significance (with a sufficiently large number of traces) and time duration to capture intermittent sources. The second aspect regards the documentation by selective measurements of the influence of the site and line, by measuring basic configurations with a switched off vehicle in pantograph down and up conditions;
- adequate scan speed to cope not only with standard requirements of sweep time, but also to limit the variability due to change of the measurement distance, as the vehicle moves. Variability has been evaluated for the measurement area extension under a far-field assumption in Section 3.1;
- wise de-synchronization of scans with respect to vehicle run and driving style to avoid weird by-products and systematic errors, that consist for example of transients persistently appearing at the same frequency bins giving the impression of an intentional source;
- recognition of line resonances amid spectral components of rolling stock emissions, based mainly on the width of the peak with respect to a truly said narrowband emission;
- evaluation of repeatability and uncertainty beyond the inadequate approach of the EN 50121 standard of considering only instrumental uncertainty, that would make site and laboratory measurements alike, as all non-ideality and external influences of a real site are de facto ignored.

Focusing on the recent widespread use of digital transmission technology for signaling and communication, in particular within the right-of-way, the inadequacy of the basic swept frequency measurement method came out, particularly considering transient electric arc emissions. APD post-processing of swept-frequency data is a first step in the direction of a better representation, but cannot solve the inherent limitations of the swept frequency method with respect to transients. A real-time spectrum analyzer can give better results, but a time-domain measurement (despite its limited dynamic range) is even more flexible and allows the contemporary analysis of different bands, as well as the analysis of the distribution of disturbance along the time axis. The repetition interval of pulsed disturbance is in fact a key parameter to assess interference to modern digital radio systems, which are characterized by increased throughput figures and negotiate channel access with tight timing. The repetition interval statistics should in general be included in the specific assessment of interference.

Funding: This research received no external funding.

Institutional Review Board Statement: Not applicable.

Informed Consent Statement: Not applicable.

Conflicts of Interest: The author declares no conflict of interest.

References

1. Mariscotti, A.; Marrese, A.; Pasquino, N.; Lo Moriello, R.S. Time and frequency characterization of radiated disturbance in telecommunication bands due to pantograph arcing. *Measurement* **2013**, *46*, 4342–4352. [CrossRef]
2. Romero, G.; Simon, E.P.; Deniau, V.; Gransart, C.; Kousri, M. Evaluation of an IEEE 802.11n Communication System in presence of Transient Electromagnetic Interferences from the Pantograph-Catenary Contact. In Proceedings of the 32nd URSI General Assembly and Scientific Symposium of the International Union of Radio Science (GASS), Montreal, QC, Canada, 19–26 August 2017. [CrossRef]
3. Geise, R.; Kerfin, O.; Neubauer, B.; Zimmer, G.; Enders, A. EMC Analysis Including Receiver Characteristics—Pantograph Arcing and the Instrument Landing System. In Proceedings of the IEEE International Symposium on Electromagnetic Compatibility, Dresden, Germany, 16–22 August 2015. [CrossRef]

4. Mauriello, A.J.; Clarke, J.M. Measurement and analysis of radiated electromagnetic emissions from rail-transit vehicles. *IEEE Trans. Electromagn. Compat.* **1983**, *25*, 405–411. [CrossRef]
5. Klapas, D.; Hackam, R.; Beanson, F.A. Electric arc power collection for high-speed trains. *Proc. IEEE* **1976**, *64*, 1699–1715. [CrossRef]
6. Wu, G.; Wu, J.; Wei, W.; Zhou, Y.; Yang, Z.; Gao, G. Characteristics of the Sliding Electric Contact of Pantograph/Contact Wire Systems in Electric Railways. *Energies* **2018**, *11*, 17. [CrossRef]
7. Midya, S.; Thottappillil, R. An overview of electromagnetic compatibility challenges in European Rail Traffic Management System. *Transp. Res. Part C* **2008**, *16*, 515–534. [CrossRef]
8. Karadimou, E.; Armstrong, R. Test of rolling stock electromagnetic compatibility for cross-domain interoperability. *IET Intell. Transp. Sys.* **2016**, *10*, 10–16. [CrossRef]
9. Pous, M.; Azpurua, M.A.; Silva, F. Measurement and Evaluation Techniques to Estimate the Degradation Produced by the Radiated Transients Interference to the GSM System. *IEEE Trans. Electrom. Comp.* **2015**, *57*, 1382–1390. [CrossRef]
10. Dudoyer, S.; Deniau, V.; Ambellouis, S.; Heddebaut, M.; Mariscotti, A. Classification of Transient EM Noise Depending on their Effect on the Quality of GSM-R Reception. *IEEE Trans. Electrom. Comp.* **2013**, *55*, 867–874. [CrossRef]
11. Boschetti, G.; Mariscotti, A.; Deniau, V. Assessment of the GSM-R susceptibility to repetitive transient disturbance. *Measurement* **2012**, *45*, 2226–2236. [CrossRef]
12. Romero, G.; Deniau, V.; Simon, E.P. Impact of the Measurement Methods on the Characterization of Transient Electromagnetic (EM) Interferences above 2 GHz in a Railway Environment. In Proceedings of the URSI Asia Pacific Radio Science Conference, New Delhi, India, 9–15 March 2019. [CrossRef]
13. Kousri, M.R.; Deniau, V.; Heddebaut, M.; Baranowski, S. Evaluation of the Impact of Transient Disturbances on Railway Signaling Systems using an Adapted Time-Frequency Analysis Method. *Arch. Electr. Eng.* **2017**, *63*, 347–354. [CrossRef]
14. Ma, L.; Wen, Y.; Marvin, A.; Karadimou, E.; Armstrong, R.; Cao, H. A Novel Method for Calculating the Radiated Disturbance from Pantograph Arcing in High-Speed Railway. *IEEE Trans. Veh. Tech.* **2017**, *66*, 8734–8745. [CrossRef]
15. Mogatadakala, K.V.; Zhang, Z. Phase errors in FSE signals due to low frequency electromagnetic interference. *Magn. Reson. Imaging* **2013**, *31*, 1384–1389. [CrossRef] [PubMed]
16. EN 50121-2 (IEC 62236-2); *Railway Applications—Electromagnetic Compatibility—Part 2: Emission of the Whole Railway System to the Outside World*; CENELEC: Brussels, Belgium, 2006.
17. EN 50121-2 (IEC 62236-2); *Railway Applications—Electromagnetic Compatibility—Part 2: Emission of the Whole Railway System to the Outside World*; CENELEC: Brussels, Belgium, 2015.
18. Pous, M.; Azpúrua, M.A.; Silva, F. Improved Electromagnetic Compatibility Standards for the Interconnected Wireless World. In Proceedings of the International Symposium on Electromagnetic Compatibility (EMC Europe), Barcelona, Spain, 2–6 September 2019. [CrossRef]
19. EN 50121-3-1 (IEC 62236-3-1); *Railway Applications—Electromagnetic Compatibility—Rolling Stock—Part 3.1: Train and Complete Vehicle*; CENELEC: Brussels, Belgium, 2006.
20. EN 50121-3-1 (IEC 62236-3-1); *Railway Applications—Electromagnetic Compatibility—Rolling Stock—Part 3.1: Train and Complete Vehicle*; CENELEC: Brussels, Belgium, 2015.
21. EN 50129; *Railway Applications—Communication, Signalling and Processing Systems—Safety Related Electronic Systems for Signalling*; CENELEC: Brussels, Belgium, 2019.
22. IEC 61508-2; *Functional Safety of Electrical/Electronic/Programmable Electronic Safety-Related Systems—Part 2: Requirements for Electrical/Electronic/Programmable Electronic Safety-Related Systems*; IEC: Geneva, Switzerland, 2011.
23. Mariscotti, A. Normative Framework for the Assessment of the Radiated Electromagnetic Emissions from Traction Power Supply and Rolling Stock. In Proceedings of the IEEE Vehicle Power and Propulsion Conference, Hanoi, Vietnam, 14–17 October 2019. [CrossRef]
24. UMTA-MA-06-0153-85-10; *Radiated Interference in Rapid Transit Systems—Volume I: Theory and Data*; Urban Mass Transport Administration: Washington, DC, USA, April 1988.
25. UMTA-MA-06-0153-85-11; *Radiated Interference in Rapid Transit Systems—Volume II: Suggested Test Procedures*; Urban Mass Transport Administration: Washington, DC, USA, June 1987.
26. Los Angeles Metro HR4000 Heavy Rail Vehicle Technical Specification Project 30433100. 2001. Available online: https://www.bidnet.com/bneattachments?/315107515.pdf (accessed on 31 May 2020).
27. Holmstrom, F.R.; Turner, D.; Fernald, E. Rail Transit EMI-EMC. *IEEE Electrom. Comp. Mag.* **2012**, *1*, 79–82. [CrossRef]
28. MIL STD 461G; *Requirements for the Control of Electromagnetic Interference Characteristics of Subsystems and Equipment*; Department of Defense: Arlington, VA, USA, 2015.
29. Rostamzadeh, C.; De Roy, P.; Barchanski, A.; Abdolali, B. Investigation of Electromagnetic Field Coupling from DC-DC Buck Converters to Automobile AM/FM Antennas. In Proceedings of the IEEE International Symposium on Electromagnetic Compatibility, Ottawa, ON, Canada, 25–29 July 2016. [CrossRef]
30. Han, D.; Li, S.; Wu, Y.; Choi, W.; Sarlioglu, B. Comparative Analysis on Conducted CM EMI Emission of Motor Drives: WBG Versus Si Devices. *IEEE Trans. Ind. Electron.* **2017**, *64*, 8353–8363. [CrossRef]

31. Ai, B.; Cheng, X.; Kürner, T.; Zhong, Z.-D.; Guan, K.; He, R.-S.; Xiong, L.; Matolak, D.W.; Michelson, D.G.; Briso-Rodriguez, C. Challenges Toward Wireless Communications for High-Speed Railway. *IEEE Trans. Intell. Transp. Sys.* **2014**, *15*, 2143–2158. [CrossRef]
32. Karimi, O.B.; Liu, J.; Wang, C. Seamless Wireless Connectivity for Multimedia Services in High Speed Trains. *IEEE J. Sel. Areas Comm.* **2012**, *30*, 729–739. [CrossRef]
33. Wang, J.; Wang, G.; Zhang, D.; Zhang, J.; Wen, Y. The Influence of Pantograph Arcing Radiation Disturbance on LTE-R. In Proceedings of the International Conference on Electromagnetics in Advanced Applications (ICEAA), Granada, Spain, 9–13 September 2019. [CrossRef]
34. García-Loygorri, J.M.; Val, I.; Arriola, A.; Briso, C. Channel Model and Interference Evaluation for a Wireless Train Backbone. *IEEE Access* **2019**, *7*, 115518–115527. [CrossRef]
35. Lin, Y.; Zhang, J.; Tan, Z.; Jin, X. Analysis on Radio Immunity of TD-LTE to Interference in High Speed Railway. In Proceedings of the International Conference on Electromagnetics in Advanced Applications (ICEAA), Granada, Spain, 9–13 September 2019. [CrossRef]
36. Laiyemo, A.O.; Pennanen, H.; Pirinen, P.; Latva-aho, M. Transmission Strategies for Throughput Maximization in High-Speed-Train Communications: From Theoretical Study to Practical Algorithms. *IEEE Trans. Veh. Tech.* **2017**, *66*, 2997–3011. [CrossRef]
37. Fraga-Lamas, P.; Fernández-Caramés, T.M.; Castedo, L. Towards the Internet of Smart Trains: A Review on Industrial IoT-Connected Railways. *Sensors* **2017**, *17*, 1457. [CrossRef]
38. Bellan, D.; Spadacini, G.; Fedeli, E.; Pignari, S.A. Space-Frequency Analysis and Experimental Measurement of Magnetic Field Emissions Radiated by High-Speed Railway Systems. *IEEE Trans. Electromagn. Compat.* **2013**, *55*, 1031–1042. [CrossRef]
39. Bellan, D.; Gaggelli, A.; Maradei, F.; Mariscotti, A.; Pignari, S. Time-Domain Measurement and Spectral Analysis of Non-Stationary Low-Frequency Magnetic Field Emissions on Board of Rolling Stock. *IEEE Trans. Electromagn. Compat.* **2004**, *46*, 12–23. [CrossRef]
40. Alonso, D.; Rull, J.; Silva, F.; Pous, M.; Coves, J.; Oriol, R. Measuring, Modeling and Correction Actions for EMC Assessment between High Speed Railway and Medical Equipment. In Proceedings of the Electrical Systems for Aircraft, Railway and Ship Propulsion (ESARS), Bologna, Italy, 19−21 October 2010. [CrossRef]
41. EN 55011; *Industrial, Scientific and Medical Equipment—Radio-Frequency Disturbance Characteristics—Limits and Methods of Measurement*; CENELEC: Brussels, Belgium, 2017.
42. EN 55022; *Information Technology Equipment—Radio Disturbance Characteristics—Limits and Methods of Measurement*; CENELEC: Brussels, Belgium, 2015.
43. Li, X.; Zhu, F.; Lu, H.; Qiu, R.; Tan, Y. Longitudinal Propagation Characteristic of Pantograph Arcing Electromagnetic Emission With High-Speed Train Passing the Articulated Neutral Section. *IEEE Trans. Electromagn. Compat.* **2019**, *61*, 319–326. [CrossRef]
44. European Radiocommunications Committee. Current and Future Use of Frequencies in the LF, MF and HF Bands. Rep. 107. Available online: https://www.ecodocdb.dk/download/5c8328b7-a746/REP107.pdf (accessed on 29 November 2020).
45. Mariscotti, A. Self and mutual capacitance of conductors in air and lossy earth with application to electrified railways. *Arch. Electr. Eng.* **2019**, *68*, 859–873. [CrossRef]
46. International Telegraph and Telephone Consultative Committee (CCITT). *Directives Concerning the Protection of Telecommunication Lines against Harmful Effects from Electric Power and Electrified Rail-Way Lines*; CCITT: Geneva, Switzerland, 1898; Volume II.
47. Mariscotti, A. Measurement Procedures and Uncertainty Evaluation for Electromagnetic Radiated Emissions from Large Power Electrical Machinery. *IEEE Trans. Instrum. Meas.* **2007**, *56*, 2452–2463. [CrossRef]
48. Ferrari, P.; Mariscotti, A.; Motta, A.; Pozzobon, P. Electromagnetic Emissions from Electrical Rotating Machinery. *IEEE Trans. Energy Conv.* **2001**, *16*, 68–73. [CrossRef]
49. CISPR 16-1-1; *Specification for Radio Disturbance and Immunity Measuring Apparatus and Methods—Part 1-1: Radio Disturbance and Immunity Measuring Apparatus—Measuring Apparatus*; IEC: Geneva, Switzerland, 2015.
50. Mariscotti, A. *RF and Microwave Measurements*, 1st ed.; ASTM: Chiasso, Switzerland, 2015.
51. CISPR 12; *Vehicles, Boats and Internal Combustion Engines—Radio Disturbance Characteristics—Limits and Methods of Measurement for the Protection of Off-Board Receivers*; IEC: Geneva, Switzerland, 2009.
52. Linkwitz, S.; Wilcox, A. Narrowband and Broadband EMI Signals using Spectrum Analyzers. In *HP RF & Microwave Measurement Symposium and Exhibition*; Hewlett Packard: Palo Alto, CA, USA, 1984.
53. Mariscotti, A. *Electromagnetic Compatibility in Railways—Electromagnetic Field Measurement*, 1st ed.; ASTM: Chiasso, Switzerland, 2016.
54. EN 50121-3-1 (IEC 62236-3-1); *Digital Cellular Telecommunications System (Phase 2+)*; Radio Transmission and Reception; European Telecommunications Standards Institute: Sophia Antipolis, France, November 2005.
55. BIPM. *Evaluation of Measurement Data—Guide to the Expression of Uncertainty in Measurement*; JCGM 100: Sèvres, France, 2008.
56. CISPR 16-4-1; *Specification for Radio Disturbance and Immunity Measuring Apparatus and Methods—Part 4-1: Uncertainties, Statistics and Limit Modelling—Uncertainties in Standardized EMC Tests*; IEC: Geneva, Switzerland, 2009.
57. Mariscotti, A.; Pozzobon, P. Synthesis of line impedance expressions for railway traction systems. *IEEE Trans. Veh. Techn.* **2003**, *52*, 420–430. [CrossRef]
58. Mariscotti, A.; Pozzobon, P. Determination of the Electrical Parameters of Railway Traction Lines: Calculation, Measurement and Reference Data. *IEEE Trans. Power Del.* **2004**, *19*, 1538–1546. [CrossRef]

59. Cintolesi, B.; Mari, M.; Mariscotti, A.; Merlo, D. Modeling the Magnetic Field Emissions from a Third Rail System. In Proceedings of the Electrical Systems for Aircraft, Railway and Ship Propulsion (ESARS), Bologna, Italy, 19−21 October 2010. [CrossRef]
60. Di Rienzo, L.; Zhang, Z.; Pignari, S.A. Boundary-Element Computation of Per-Unit-Length Series Parameters of Railway Lines. *IEEE Trans. Electromagn. Compat.* **2009**, *51*, 825–832. [CrossRef]
61. Mariscotti, A.; Pozzobon, P. Measurement of the Internal Impedance of Traction Rails at Audiofrequency. *IEEE Trans. Instr. Meas.* **2004**, *53*, 792–797. [CrossRef]
62. Schaefer, W. Understanding impulse bandwidth specifications of EMI receivers. In Proceedings of the IEEE International Symposium on Electromagnetic Compatibility, Symposium Record, Seattle, WA, USA, 2–6 August 1999. [CrossRef]
63. Pous, M.; Azpúrua, M.A.; Oliva, J.A.; Aragón, M.; González, I.; Silva, F. Full Time Domain EMI measurement system applied to Railway emissions according to IEC 62236-3-1/EN 50121-3-1 standards. In Proceedings of the International Symposium on Electromagnetic Compatibility (EMC Europe), Amsterdam, The Netherlands, 27–30 August 2018. [CrossRef]
64. Agilent Technologies, PSA Series Spectrum Analyzers—Specifications Guide. E4440-90647, December 2012. Available online: https://literature.cdn.keysight.com/litweb/pdf/E4440-90647.pdf (accessed on 26 July 2020).
65. Sander, K.U. Speed Considerations for Spurious Level Measurements with Spectrum Analyzers. Rohde-Schwarz, 1EF80-1E, July 2012. Available online: https://scdn.rohde-schwarz.com/ur/pws/dl_downloads/dl_application/application_notes/1ef80/1EF80_1E.pdf (accessed on 26 November 2020).
66. Harris, F.J. On the use of windows for harmonic analysis with the discrete Fourier transform. *Proc. IEEE* **1978**, *66*, 51–83. [CrossRef]
67. Sandrolini, L.; Mariscotti, A. Impact of Short-Time Fourier Transform Parameters on the Accuracy of EMI Spectra Estimates in the 2–150 kHz Supraharmonic Interval. *Electr. Power Sys. Res.* **2021**. in review.
68. Sandrolini, L.; Mariscotti, A. Signal Transformations for Analysis of Supraharmonic EMI Caused by Switched-Mode Power Supplies. *Electronics* **2020**, *9*, 2088. [CrossRef]
69. Wiklundh, K. Relation between the amplitude probability distribution of an interfering signal and its impact on digital radio receivers. *IEEE Trans. Electromagn. Compat.* **2006**, *28*, 537–544. [CrossRef]
70. Matsumoto, Y.; Gotoh, K. An expression for maximum bit error probability using the amplitude probability distribution of an interfering signal and its application to emission requirements. *IEEE Trans. Electromagn. Compat.* **2013**, *55*, 983–986. [CrossRef]
71. Pous, M.; Silva, F. Full-Spectrum APD Measurement of Transient Interferences in Time Domain. *IEEE Trans. Electrom. Comp.* **2014**, *56*, 1352–1360. [CrossRef]
72. Geng, X.; Wen, Y.; Zhang, J.; Zhang, D. A Method to Supervise the Effect on Railway Radio Transmission of Pulsed Disturbances Based on Joint Statistical Characteristics. *Appl. Sci.* **2020**, *10*, 4814. [CrossRef]
73. Geng, X.; Wen, Y.; Zhang, J. An APD-Based Evaluation on the Effect of Transient Disturbance over Digital Transmission. *Chin. J. Electron.* **2020**, *29*, 57–65. [CrossRef]
74. Chiyojima, T. Introduction of the amplitude probability distribution (APD) measurement in CISPR 32. In Proceedings of the Joint International Symposium on Electromagnetic Compatibility, Sapporo and Asia-Pacific International Symposium on Electromagnetic Compatibility (EMC Sapporo/APEMC), Sapporo, Japan, 3–7 June 2019. [CrossRef]
75. EN 55032; *Electromagnetic Compatibility of Multimedia Equipment—Emission Requirements*; CENELEC: Brussels, Belgium, 2015.
76. Mariscotti, A. Assessment of Electromagnetic Emissions from Synchronous Generators and its Metrological Characterization. *IEEE Trans. Instrum. Meas.* **2010**, *59*, 450–457. [CrossRef]